Veterinary Microbiology 172 (2014) 129–139

Contents lists available at ScienceDirect

Veterinary Microbiology

journal homepage: www.elsevier.com/locate/vetmic

Virion-associated viral proteins of a Chinese giant salamander (*Andrias davidianus*) iridovirus (genus *Ranavirus*) and functional study of the major capsid protein (MCP)

Wei Li [a], Xin Zhang [b], Shaoping Weng [a], Gaoxiang Zhao [b], Jianguo He [a,c], Chuanfu Dong [a,*]

[a] State Key Laboratory for Biocontrol, School of Life Sciences, Sun Yat-sen University, 135 Xingang Road West, Guangzhou 510275, PR China
[b] Department of Biology, Jinan University, Guangzhou 510632, PR China
[c] School of Marine Sciences, Sun Yat-sen University, 135 Xingang Road West, Guangzhou 510275, PR China

ARTICLE INFO

Article history:
Received 9 November 2013
Received in revised form 1 May 2014
Accepted 4 May 2014

Keywords:
Chinese giant salamander iridovirus
Proteomics
Virion protein
Major capsid protein (MCP)
siRNA
Neutralization test

ABSTRACT

Chinese giant salamander iridovirus (CGSIV) is the emerging causative agent to farmed Chinese giant salamanders in nationwide China. CGSIV is a member of the common midwife toad ranavirus (CMTV) subset of the amphibian-like ranavirus (ALRV) in the genus *Ranavirus* of Iridoviridae family. However, viral protein information on ALRV is lacking. In this first proteomic analysis of ALRV, 40 CGSIV viral proteins were detected from purified virus particles by liquid chromatography-tandem mass spectrometry analysis. The transcription products of all 40 identified virion proteins were confirmed by reverse transcription polymerase chain reaction analysis. Temporal expression pattern analysis combined with drug inhibition assay indicated that 37 transcripts of the 40 virion protein genes could be classified into three temporal kinetic classes, namely, 5 immediate early, 12 delayed early, and 20 late genes. The presence of major capsid proteins (MCP, ORF019L) and a proliferating cell nuclear antigen (ORF025L) was further confirmed by Western blot analysis. The functions of MCP were also determined by small interfering RNA (siRNA)-based knockdown assay and anti-recombinant MCP serum-based neutralization testing. At low dosages of CGSIV, siRNA-based knockdown of the MCP gene effectively inhibited CGSIV replication in fathead minnow cells. The antiviral effect observed in the anti-MCP serum-based neutralization test confirms the crucial function of the MCP gene in CGSIV replication. Taken together, detailed information on the virion-associated viral proteins of ALRV is presented for the first time. Our results also provide evidence that MCP is essential for CGSIV replication *in vitro*.

1. Introduction

Piscine iridovirus is a large double-stranded DNA virus, which mainly comprises the genera *Ranavirus*, *Lymphocystivirus*, and *Megalocytivirus* in the Iridoviridae family; this virus can infect a wide range of cold-blooded low vertebrates (Jancovich et al., 2012). Among piscine iridoviruses, lymphocystivirus and megalocytivirus can only infect certain kinds of bony fishes, whereas ranavirus has a broader and global range of low vertebrate host species, including fishes, amphibians, and reptiles (Chinchar and Waltzek, 2014; Whittington et al., 2010). As of this writing, well-known ranaviruses, such as frog virus 3 (FV3) (Tan et al., 2004), *Ambystoma tigrinum* virus

* Corresponding author: Tel.: +86 2084113793; fax: +86 2084113229.
E-mail address: dongchfu@mail.sysu.edu.cn (C. Dong).

http://dx.doi.org/10.1016/j.vetmic.2014.05.009
0378-1135/

(ATV) (Jancovich et al., 2003), tiger frog virus (TFV) (He et al., 2002), soft-shelled turtle iridovirus (STIV) (Huang et al., 2009), *Rana grylio* virus (RGV) (Lei et al., 2012), epizootic hematopoietic necrosis virus (EHNV) (Jancovich et al., 2010), European sheatfish ranavirus (ESV/ECV) (Mavian et al., 2012b), Singapore grouper iridovirus (SGIV) (Song et al., 2004), and grouper iridovirus (GIV) (Tsai et al., 2005), have been associated with mortality events in ecologically and economically important bony fishes, amphibians, and reptiles; these viruses have been fully sequenced and widely studied (Chinchar et al., 2011).

Recently, a new common midwife toad ranavirus (CMTV) reportedly causes fetal diseases in several amphibian species across Europe (Mavian et al., 2012a). Mavian et al. proposed that CMTV represents an intermediate in the amphibian-like ranavirus (ALRV) evolution. In the meantime, CMTV-close ranaviruses have also been isolated and identified from infected farmed Chinese giant salamanders (*Andrias davidianus*) in different areas in China and were designated as Chinese giant salamander virus (CGSV) (Geng et al., 2011), *A. davidianus* iridovirus (Jiang et al., 2011), and *A. davidianus* ranavirus (Chen et al., 2013). Clinical signs of infection include skin ulceration, anorexia, lethargy, occasionally edema, petechiae, erythema, toe necrosis, friable and gray–black liver, and friable lesions of the kidney and spleen. Morbidity could be higher than 95% in some affected areas (Dong et al., 2011b). In 2011, we isolated a Chinese giant salamander iridovirus (CGSIV strain HN11) from diseased farmed Chinese giant salamanders in Zhangjiajie National Forest Park, Hunan Province, China, and determined and annotated the complete genome sequence of CGSIV-HN11 (Accession number: KF512820).

Ranaviruses can be subdivided into two distinct groups according to 26 conserved core iridoviral proteins-based phylogenetic analyses and genome collinearity; these groups include GIV-like ranaviruses (GLRV) and ALRV (Jancovich et al., 2010). The GLRV group includes GIV and SGIV, which specifically infect marine-cultured groupers (*Epinephelus* sp.), as reported in Singapore and Chinese Taiwan (Song et al., 2004; Tsai et al., 2005). ALRVs mainly comprise well-known viruses such as FV3, ATV, TFV, RGV, CMTV, EHNV, ESV, and STIV; the natural hosts of these viruses include a wide range of cold-blooded vertebrates, such as fish, reptiles, amphibians, and turtles (Mavian et al., 2012a). Within the ALRV group, three different subsets can be distinguished: EHNV/ATV/ESV, FV3/TFV/STIV, and CMTV (Mavian et al., 2012a). Conserved core iridoviral protein-based phylogenetic analyses and genome collinearity analysis show that CGSIV-HN11 is a member of the CMTV subset in ALRV (data not shown).

Viral structural proteins have crucial functions in viral bioprocesses, including structure formation and scaffolding of virus particles, virus–host interactions, initial steps in virus infection, transcription of viral genes, early-stage DNA replication, and host shifts (Whitley et al., 2010). As of this writing, 22 piscine iridoviruses, including 13 ranaviruses, 7 megalocytiviruses, and 2 lymphocystiviruses, have been fully sequenced. However, the virion proteins of only one GLRV-like ranavirus and two megalocytiviruses have been comprehensively determined and reported (Dong et al., 2011a; Shuang et al., 2013; Song et al., 2006). The functions of most viral proteins remain unclear, which greatly limits the understanding of the viral biological process in piscine iridovirus (Chinchar et al., 2011).

In this work, we report the proteomic analysis of CGSIV-HN11 virions. The functional profiles of MCP in *in vitro* cell models of *Epithelioma papulosum cyprini* (EPC) cells and fathead minnow muscle (FHM) cells were evaluated. A better understanding of structural proteins and their localization in the virions will contribute to future studies on ranavirus assembly and infection pathways and the discovery of vaccine candidates for CGSIV and other piscine iridoviruses.

2. Materials and methods

2.1. Ethics statement

Animal handling was conducted according to the recommendations in the Regulations for the Administration of Affairs Concerning Experimental Animals of China. The protocol was approved by the Animal Care and Use Committee of Sun Yat-Sen University, and all efforts were made to minimize the suffering of the animals.

2.2. Virus and cell line

The virus strain CGSIV-HN2011 was isolated from a diseased Chinese giant salamander obtained in Zhangjiajie National Forest Park in late June 2011 using EPC cells. EPC cells were maintained in M199 growth medium containing 10% fetal bovine serum (FBS), 100 IU/mL penicillin, and 100 μg/mL streptomycin at 27 °C. Induced cytopathic effects (CPE) in infected EPC cells were observed at regular intervals. When advanced CPE had occurred, the virus was harvested and stored at −80 °C for further use.

2.3. Purification of virus and virion-associated viral proteins by liquid chromatography–electrospray tandem mass spectrometry (LC ESI–MS/MS)

Frozen infected EPC cells were freeze-thawed thrice to release the CGSIV. The cell debris was pelleted at 10,000 × *g* for 30 min at 4 °C, and the cell-free supernatant was centrifuged at 150,000 × *g* in a Beckman type 70 Ti rotor for 30 min at 4 °C. The virus pellet was resuspended in TNE buffer with 50 mM Tris–HCl, 150 mM NaCl, and 1 mM disodium ethylenediaminetetraacetic acid (EDTA) at pH 7.4 and 4 °C. The pellet was carefully layered onto a linear 30–60% (w/v) continuous sucrose gradient. After 2 h of centrifugation at 150,000 × *g* at 4 °C in a Beckman SW40 Ti rotor, the viral band from the 50% sucrose layer was collected and resuspended in TNE buffer. Virion pellets were harvested after centrifugation at 150,000 × *g* and 4 °C for 30 min and suspended in TN buffer with 50 mM Tris–HCl and 150 mM NaCl at pH 7.4 and 4 °C). Viral purity was determined using transmission electron microscopy (TEM).

Viral particles were suspended in approximately 5 volumes of 0.1% SDS and 50 mM Tris–HCl (pH 8.5) and

incubated at 100 °C with intermittent vortex mixing until the viscous lump had disappeared. After centrifugation, the supernatant was retrieved. Extracted proteins were separated by 12.5% SDS-PAGE, and the gel lane with the separated viral proteins was excised as three fractions and subjected to in-gel digestion. Digested peptides were subjected to high performance LC–ESI–MS/MS analysis at the Research Center for Proteome Analysis (Shanghai, China), as previously described (Shuang et al., 2013). Peptides were solubilized in 20 μL of mobile phase A [2% (v/v) acetonitrile and 0.1% (v/v) formic acid], and 5 μL was injected into Zorbax 300SB-C18 peptide traps (Agilent Technologies, Wilmington, DE) and loaded into a 0.15 mm × 150 mm C18 reverse phase LC column (Column Technology, Inc.). The reverse phase gradient was 0.1% formic acid in acetonitrile (84%). The reverse phase gradient concentration in a linear gradient was increased from 4% to 50% in 50 min and from 50% to 100% in 4 min followed by 100% for 6 min. The eluted peptides were desalted and directly introduced into an ESI–linear ion trap–mass spectrometer (LTQ VELOS, Thermo Finnegan, San Jose, CA, USA) set in positive ion mode. The microspray temperature was set to 200 °C for peptides. After obtaining a full scan of the mass spectra, three MS/MS scans were acquired for the next three most intense ions using dynamic exclusion. The resulting mass spectra were analyzed using Sequest software against uniprot_Ranavirus_20130313_1481.fasta.

2.4. Temporal transcription analysis

The presence of a transcript for each of the 40 virion genes in the CGSIV-HN11 genome was tested by RT-PCR. Monolayer EPC cells were infected or mock-infected with CGSIV-HN11 at a multiplicity of infection (MOI) of 1 and harvested at 2, 6, and 48 h post infection (hpi). RNA was extracted using TRIzol® Reagent (Life Technologies, USA) according to the manufacturer's description. RNA was reverse transcribed into cDNA using an Access reverse transcription polymerase chain reaction (RT-PCR) system kit (Promega, USA). Random decamer primers were added subsequently. Semi-quantitative PCRs were performed using an 18S rRNA gene primer set (18SF: 5′-ATGGTACTTTAGGCGCCTAC-3′, 18SR: 5′-TATACGCTATTGGAGCTGG-3′, 280 bp). The specific primers and product sizes for the viral genes of CGSIV-HN11 are listed in Table 2. For time course studies, viral RNA was isolated from mock- and virus-infected cells at 0, 2, 4, 6, 8, 12, 18, 24, 48, and 72 hpi. To classify the transcripts into temporal kinetic classes, RNA samples were isolated from CGSIV-HN11-infected cells under different drug inhibition conditions. Cycloheximide (CHX; Sigma, USA), a *de novo* protein synthesis inhibitor, and cytosine arabinofuranoside (AraC; Sigma), a viral DNA replication inhibitor, were selected as inhibitory drugs. EPC monolayer cells were pretreated with CHX (200 μg/mL) or AraC (100 μg/mL) for 1 h prior to and during CGSIV-HN11 infection. CHX-pretreated cells and AraC-pretreated cells were mock-infected or infected with CGSIV-HN11 at approximately 1 MOI. CHX-pretreated cells were then harvested at 6 hpi, whereas AraC-pretreated cells were harvested at 48 hpi. RNA isolation and RT-PCR analysis were performed following the treatment described above. Each PCR fragment was confirmed to be a single band with the correct size by running on 1.5% or 2% agarose gel. Amplified fragments were confirmed by sequencing.

2.5. Prokaryotic expression, purification, and antibody preparation of recombinant viral proteins

Major capsid protein (MCP; CGSIV-ORF019L) and proliferating cell nuclear antigen (PCNA, CGSIV-ORF025L) genes were amplified from CGSIV-HN11 genomic DNA using two primer sets, as follows: MCP-F: 5′-GGAATTC-**CATATG**TCTTCTGTAACGGGTTCAGG-3′, MCP-R: 5′-ATAAGAAT**GCGGCCGC**CAAGATTGGGAATCCCATCG-3′; PCNA-F: 5′-GGAATTC**CATATG**CTGTGGGAAGCCGTA-3′; PCNA-R: 5′-ATAAGAATGCG**GCCGCGC**CCTCAAAGAGAGTCACG-3′. Here, restriction enzyme sequences are in bold and underlined. PCR fragments for MCP and PCNA were directionally cloned into plasmid pET22b(+), digested with the corresponding enzyme (*NdeI-NotI*), and expressed in *Escherichia coli* Rosetta™ (DE3). Cell suspensions were disrupted by sonication in an ice bath and centrifugation at 10,000 × *g* for 10 min at 4 °C. Supernatants containing recombinant proteins were subsequently purified by affinity chromatography on nickel–nitrilotriacetic acid Superflow resin (Qiagen, Germany) according to the manufacturer's instructions. Purified recombinant viral proteins were emulsified with equal volumes of Freund's complete adjuvant (Sigma) for the first injection and Freund's incomplete adjuvant (Sigma) for the next three booster immunizations. The mice received the four subcutaneous injections at one-week intervals. Anti-sera were collected at the 7th day after the last injection.

2.6. Time courses and localization of MCP and PCNA in CGSIV virions by Western blot (WB) analysis

EPC cells were grown in 25 cm^2 tissue culture flasks until 90% confluence and subsequently infected with the CGSIV-HN11 suspension (MOI = 1). After incubation for 1 h at 27 °C, the growth medium was replaced with the maintenance medium (M199 + 2.5% FBS). Infected cells were digested by 0.25% trypsin-EDTA solution and collected by centrifugation at 800 × *g* for 5 min at room temperature (RT) at 0, 2, 6, 12, 24, 48, and 72 hpi. After rinsing with sterile phosphate-buffered saline (PBS) for 3 min at RT, the total cellular proteins were extracted using lysis buffer. The protein concentration was determined by the Bradford method according to the guidelines in the operating manual. The total proteins were separated by 12% SDS-PAGE and subjected to WB analysis. Mouse anti-sera against recombinant MCP and PCNA were used as first antibodies.

To confirm the localizations of MCP and PCNA in CGSIV virions, the purified virus suspension was separated by 12% SDS-PAGE. Proteins obtained were then transferred onto nitrocellulose (NC) membranes (Whatman, UK) under a constant current of 200 mA for 2 h. The NC membranes were blocked with 5% fat-free milk in Tris-buffered saline (TBS) comprising 0.02 M Tris–HCl, 0.5 M NaCl; pH 7.5) at RT for 1 h. After washing with TBS-T (0.05% Tween-20 in

TBS) thrice for 10 min each time, the membranes were incubated with mouse anti-MCP and -PCNA sera (1:1000 dilution in 5% fat-free milk), respectively, at 4 °C overnight. The membranes were then washed thrice with TBS-T (10 min for each wash) followed by incubation with the goat anti-mouse IgG-conjugated alkaline phosphatase (Sigma, USA) as a secondary antibody (1:3000 dilution). Finally, membranes were washed thrice with PBS with 0.2% Triton X-100 (PBST) and visualized in fresh nitro blue tetrazolium/5-bromo-4-chloro-3-indolyl-phosphate (NBT/BCIP) substrate solution.

2.7. Knockdown of MCP

siRNA (siR-MCP) sequences targeting the MCP transcript and a mutated siRNA (the corresponding mismatched siRNA of siR-MCP and MsiR-MCP) were designed using an algorithm supplied by the manufacturer and purchased from Guangzhou RiboBio Co., Ltd. Two non-silencing siRNA sequences were used as negative controls to monitor transfection efficiency as follows: a fluorescein-tagged non-silencing control (Qiagen, Germantown, MD) and a control siRNA that does not target any known sequence (nsRNA).

FHM cells were seeded at ~50% confluency (1×10^6 cells/well in 6-well dishes) in M199 plus 10% FBS and incubated in a humidified incubator at 27 °C. FHM cells were transfected for 24 h after plating with media containing 40 nM siRNA using Lipofectamine reagent (Invitrogen, USA). DharmaFECT 1 (Dharmacon) was used as the transfection reagent. Details of RNA interference and virus infection were described by Whitley et al. (2011). After virus adsorption for 1 h, non-attached viruses were removed by washing, and the cultures were incubated as described above. The infection was stopped at 24 and 48 hpi, and the processed replicate cultures were subjected to WB analysis, TEM observation, and plaque assay, respectively. siRNA-transfected and CGSIV-infected cells were collected. Total proteins were extracted using 100 mL of lysis buffer for WB. Anti-sera against MCP, PCNA, and β-actin were used as first antibodies. siRNA-transfected and virus-infected FHM cells were analyzed by TEM as previously described (Xie et al., 2005).

2.8. Neutralization test with anti-recombinant CGSIV-MCP serum

Virus neutralization assay was performed as described previously with some modifications (Dong et al., 2013). An equal volume of two fold dilutions of anti-recombinant MCP serum was added to the virus dilution (MOI = 1) and incubated at 24 °C for 1 h. Sera from non-immunized mice and mice treated with growth medium alone were also included in the virus dilution analysis as controls. After incubation, the mixtures were inoculated into EPC cells in 24-well plate at 300 μL per well and allowed to absorb at 24 °C for 1 h. Inoculation was done in triplicate. Another 1.7 mL of growth medium with 5% FBS was added to each well, and the cells were incubated at 27 °C for 3 d to examine CPEs. Viral supernatants of five different time-interval groups in different treatments were diluted from 10^{-1} to 10^{-8} and used to infect EPC cells with four repetitions per dilution in the $TCID_{50}$ assay. Infectious spleen and kidney necrosis virus (ISKNV) was used as a negative control as descripted previously (Dong et al., 2013). Viral titers were calculated according to the method described by Reed and Muench (1938).

3. Results

3.1. Virion-associated viral proteins in CGSIV-HN11

CGSIV-HN11 proliferated well in EPC cells. The viral titer was as high as $10^{8.5}$ $TCID_{50}$/mL at 3 d after infection treatment. Purified virions were obtained following continuous gradient sucrose-based ultracentrifugation. TEM observation showed that purified virions are approximately 150 nm in diameter with clear structural layers (Fig. 1A). The viral proteins were fractionated by 12% SDS-PAGE. Approximately 25 bands ranging from 10 kDa to 180 kDa were visualized by Coomassie brilliant blue staining (Fig. 1B). The stained gel was excised into three fractions and subjected for further LC ESI-MS/MS analysis. A total of 40 proteins were matched to the CGSIV-HN11 protein database; 16 of these proteins are core iridoviral proteins of the family *Iridoviridae* (Table 1). The homologs of all 40 virion proteins were also found in CMTV proteins database (data not shown). Compared with three virion protein-determined vertebrate iridoviruses (Dong et al., 2011a; Shuang et al., 2013; Song et al., 2006), 38, 19, and 21 of these proteins yielded homologs with predicted open reading frames (ORFs) in SGIV (another subset in Ranavirus), ISKNV, and red seabream iridovirus (RSIV) (two members of genus *Megalocytivirus*), respectively. Moreover, 26, 11, and 13 of these proteins were identified as virion proteins in SGIV, ISKNV, and RSIV (strain SKIV-ZJ07), respectively. Compared with two virion protein-determined invertebrate iridoviruses belonging to the

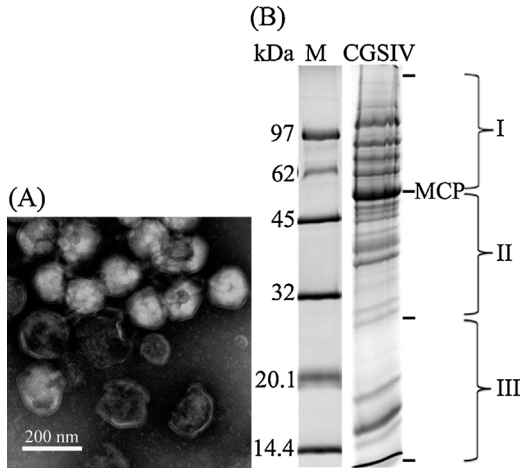

Fig. 1. Virion profiles of purified CGSIV-HN11. (A) TEM of purified CGSIV-HN11 subjected to continuous sucrose gradient-based ultracentrifugation (Bar = 200 nm); (B) polypeptide profiles of CGSIV virions separated by 12.5% SDS-PAGE. The gel was excised into three fractions (I, II, and III) and subjected to LC–ESI–MS/MS analysis. M: protein marker. Arrow indicates MCP.

Table 1
Virions-associated viral proteins of CGSIV-HN11 identified by LC–ESI–MS/MS.

No.	CGSIV-HN11 ORF	Predicted function and conserved domain[a]	MW (kDa)/PI	Unique peptides	% Cov (95)	Homology to iridovirus ORFs[b]					Other ranavirus
						SGIV	ISKNV	RSIV[c]	IIV6	IIV9	
1	002L	Myristylated membrane protein	37.9/8.44	6	21.56	019R+	90L	575R	337L+	031R+	TFV-001L+
2	003L	Hypothetical protein	32.6/7.74	5	22.22	018R+	NA	NA	NA	NA	
3	004R	Hypothetical protein	44.4/5.68	6	21.29	016L+	NA	NA	229L+	084R+	
4	005R	Hypothetical protein	6.6/9.57	1	15.00	015L+	NA	NA	NA	NA	
5	010L	SNF2 NTPase	106.3/8.19	9	11.50	060R+	63L+	63R+	022L+	055L+	
6	018L	Immediate early protein ICP-46	45.5/6.05	4	12.25	162L+	115R+	458L+	393L	059R	FV3-91R+
7	019L	Major capsid protein	50.0/5.97	14	48.60	072R+	006L+	380L+	274L+	010R+	
8	020L	Hypothetical protein	40.3/9.37	1	3.09	071R	NA	NA	NA	NA	
9	021L	Thiol oxidoreductase	16.6/8.95	2	15.33	070R+	043L+	156R+	347L	134L+	
10	022R	Hypothetical protein	65.3/10.13	12	21.60	069L+	NA	NA	NA	NA	KRV-1
11	024L	Thymidine kinase	22.2/5.06	3	21.54	067L+	032R	234L	143R	098R	
12	025L	Proliferating cell nuclear antigen	26.1/7.67	1	9.39	068L	112R+	487L+	436R	053R	
13	026L	Cytosine DNA methyltransferase	24.9/8.95	1	6.07	NA	046R	140R	NA	NA	
14	031R	Ribonuclease III	40.6/8.61	10	22.91	084L+	087R	596L	142R+	034L+	
15	036R	Lipopolysaccharide-induced TNF-alpha factor	9.3/7.04	1	8.33	136R	NA	NA	NA	NA	
16	037R	Hypothetical protein	41.8/11.36	4	16.36	137R+	NA	NA	NA	NA	
17	038R	Putative NTPase/helicase	39.2/8.08	1	5.86	146L+	NA	NA	NA	NA	
18	054L	Neurofilament triplet H1-like protein	12.6/12.26	2	40.74	022L+	NA	318R	NA	NA	
19	055L	Hypothetical protein,	15.6/8.12	1	10.14	024L	NA	NA	NA	NA	
20	057L	Putative SAP domain-containing protein	57.0/5.16	1	8.03	025L+	NA	NA	NA	NA	RGV-50L+
21	058R	Hypothetical protein	61.6/5.81	10	25.49	026R+	NA	NA	NA	NA	
22	060R	Myristylated membrane protein	50.7/6.15	11	30.46	088L+	007L+	374R+	118L+	005R+	FV-53R; RGV-53R
23	065R	Serine/threonine protein kinase	53.6/6.74	3	8.43	150L	013R	349L	098R	058L+	
24	067L	LCDV orf 88-like protein	15.6/5.82	3	37.50	021L	NA	NA	374R+	141R+	
25	069L	Orf2-like protein	129.2/8.47	7	8.58	057L+	076L+	639R+	295L+	143L+	
26	073L	Ribonucleoside diphosphate reductase α subunit	62.2/7.91	1	5.51	064R	NA	NA	NA	NA	
27	074L	NIF-NLI interacting factor	23.7/10.44	6	37.32	061R+	005L	385R+	355R+	036L+	
28	080L	L-Protein-like protein	11.4/6.86	1	20.75	009L+	NA	NA	NA	NA	
29	082L	Neurofilament triplet H1-like protein	76.5/10.06	7	15.68	012L+	NA	NA	NA	NA	FV3- 32R+
30	087L	Putative tyrosine protein kinase	107.2/8.12	8	9.28	078L+	114L	396R+	179R+	016R+	
31	089L	Early p31K protein	34.7/8.22	10	38.70	006R+	118L+	112L+	NA	110R	
32	092L	D5 NTPase	108.9/6.81	1	1.64	052L	109L+	493R+	184R	120R	
33	095L	Hypothetical protein	16.0/9.24	2	34.46	038L+	NA	407R	117L+	183R+	TFV-020R+
34	096L	Serine/threonine-protein kinase	101.8/9.43	8	12.10	039L+	55L+	106R+	380R+	023L+	
35	099R	Hypothetical protein	53.4/7.07	23	57.57	043R+	NA	NA	NA	NA	
36	103L	AAA-ATPase	35.5/5.53	4	16.46	134L	122R+	412L+	075L	079R+	
37	107R	Hypothetical protein	32.9/7.45	2	8.75	118R	096L	550R	287R	022R	
38	108L	Hypothetical protein	7.9/4.71	1	42.86	103R	NA	NA	NA	NA	
39	110R	Hypothetical protein	24.8/5.23	3	17.98	111R	NA	NA	NA	NA	
40	111R	Myeloid cell leukemia protein	15.3/5.17	1	8.03	NA	NA	NA	NA	NA	

NA: no applicable ORF.
+: Have been detected as virons proteins.
[a] Function and conserved domain were predicted by online predication tool of http://smart.embl-heidelberg.de/smart/change_mode.pl.
[b] Vrions proteins of these five iridoviruses have been determined previously.
[c] according to RSIV-type megalocytiviral strain SKIV-ZJ07 (Shuang et al., 2013).

genus *Iridovirus* (Ince et al., 2010; Wong et al., 2011), 20 homologous virion proteins were found in inveterate iridovirus type 6 and 9 (IIV6 and IIV9) (Table 1), of which 12 and 15, respectively, were previously identified as virion proteins, respectively (Ince et al., 2010; Wong et al., 2011).

PCNA was determined as a virion protein only by megalocytiviral proteomic analysis (Spotted knifejaw iridovirus strain ZJ07, SKIV-ZJ07) (Shuang et al., 2013). MCP is the most abundant protein among iridovirus particles. To further confirm the identity these two viral

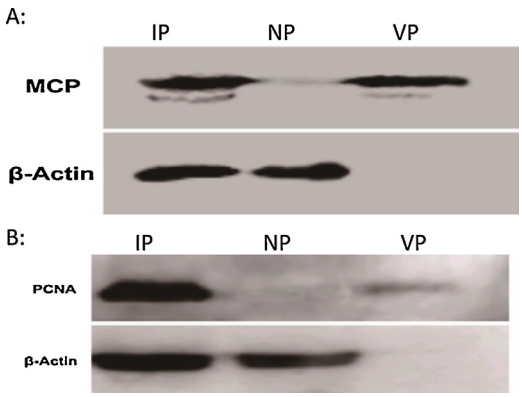

Fig. 2. Detection of MCP and PCNA in purified CGSIV virions by WB analysis. Purified CGSIV was separated by SDS-PAGE. (A) MCP was detected using anti-MCP serum by WB. (B) PCNA was detected using anti-PCNA serum by WB. IP: protein products from CGSIV-infected EPC cells at 24 hpi. NP: protein products from mock-infected EPC cells. VP: purified CGSIV virions.

proteins, anti-sera against recombinant MCP and PCNA (rMCP and rPCNA) were prepared. WB analysis showed that both MCP and PCNA could be detected specifically in purified CGSIV virions by anti-rMCP and rPCNA sera (Fig. 2), which confirms that both MCP and PCNA are viral structural proteins in CGSIV virions. By contrast, β-actin is an abundant cytoskeletal protein that can be detected in infected and mock-infected EPC cells but not in purified CGSIV (Fig. 2). Thus, β-actin is not a virion component in CGSIV.

3.2. Temporal class of the virion proteins as determined by drug inhibition assay

Iridovirus gene expression was temporally regulated, leading to the expression of three sequentially synthesized classes of genes: immediate early (IE), delayed early (E), and late (L) (Chinchar et al., 2011). The presence and temporal class of transcripts for each of the 40 virion proteins were tested in different RNA samples, including mock-infected, infected, and CHX- or AraC-treated (harvested at different time points), by RT-PCR. The transcripts of all 40 CGSIV virion protein genes were confirmed by RT-PCR with the specific primers (Table 2). In total, 37 of 40 transcripts could be classified into three temporal kinetic classes, as follows: 5 IE, 12 E, and 20 L transcripts. The remaining three viral genes are ORF-054L, -057L, and -110R.

CGSIV-MCP and CGSIV-PCNA were temporally classified as L and E viral genes, respectively, by drug inhibition assay (Table 2). To further confirm their temporal classes at the protein level, the time courses of MCP and PCNA expressions in CGSIV-infected and mock-infected EPC cells at different post-infection time intervals (0, 2, 4, 6, 8, 12, 24, 48, and 72 hpi) were determined by WB analysis. Both MCP and PCNA were highly expressed after 24 hpi (Fig. 3A). PCNA was detected as early as 6 hpi, whereas MCP was detected as early as 8 hpi. The times of expression of the proteins were consistent with their temporal class results, as determined by drug inhibition assay-based transcriptional analysis.

3.3. Inhibition of MCP gene in CGSIV-infected FHM by RNA interference

To determine MCP function in CGSIV replication, MCP target siRNA sequences were designed to block MCP expression in FHM cells (Table 3). siRNA-mediated silencing was performed in CGSIV-infected FHM cells. At 24 and 48 h post transfection, infected FHM cell proteins were extracted for WB analysis. siRNAs could effectively downregulate MCP expression in transiently transfected FHM cells. In contrast to the effectively downregulated MCP expression observed, stable expressions of PCNA and β-actin were observed at 24 and 48 h post transfection in siR-MCP and MsiR-MCP (Fig. 3B). To confirm the effect of gene silencing on viral replication, we assayed the resulting virus yields from both controls and siR-MCP-treated cultures at ~48 hpi. As shown in Fig. 4, an inhibitory effect was observed under infection with siR-MCP-treated CGSIV at an MOI of 0.4 pfu/cell in the plaque assay. Resulting virus yields from the culture infected with anti-MCP-siRNA were reduced to ~28% in the control-treated cultures (Fig. 4), which indicates that MCP may be involved in the assembly of viral particles. The reduction in MCP expression levels correlated with the reduction in infectious viral particle production.

The effect of siR-MCP treatment was examined further by TEM observation. CGSIV-infected cells treated with a control MsiRNA showed abundant virion formation. Virus particles were present at virus assembly sites and paracrystalline arrays and showed budding from the plasma membrane (Fig. 5A). By contrast, cells treated with siR-MCP showed a marked reduction in virion formation, and the presence of aberrant structures was similar to atypical elements seen in CGSIV-infected cells (Fig. 5B). Thus, MCP is confirmed to be critically involved in viral replication, assembly, and maturation.

3.4. Virus-neutralizing activity during CGSIV infection of the MCP-specific antibody

The antivirus effect of antiserum of CGSIV-MCP was detected within 72 h by an *in vitro* neutralization test. After incubation with antiserum, CGSIV mixtures were inoculated into EPC cells at an MOI of 0.4. Special antiserum-processed virus neutralizing activity was observed starting from 12 hpi (Fig. 6). The protective effects of antiserum on virus-infected cells could limit viral entry and reduce or eliminate the spread of progeny by binding with MCP. Serum from the non-immunized mice failed to prevent the growth of the virus-infected cells (Fig. 6), and growth medium alone showed no effect on the growth of infected cells (data not shown). In comparison with the CGSIV virus infection control, the appearance of CPE was obviously delayed in EPC cells inoculated with a mixture of CGSIV and anti-MCP serum after 36 hpi. However, the antiserum against CGSIV-MCP did not suppress ISKNV replication (data not shown), which indicates that the antiserum of CGSIV-MCP is specific for CGSIV but fails to show cross-

Table 2
Temporal class of 40 detected virions proteins by transcriptional analysis combination with drugs inhibition assays.

No.	ORF	Temporal class	Forward primer(F) (5′ → 3′); Reverse primer (R) (5′ → 3′)	PCR product size (bp)
1	002L	L	F: AGCACTGATCGGGGTAGGCGTGGAG R: AGGGGCACCTGCGGCAAGGACTG	517
2	003L	E	F: CAAACTCCTTGACGGGGAACATC R: CACCGCAACTCTTTCAGGCTCTAC	279
3	004R	L	F: GGAAGGTTCCAGCCGTAG R: CATCACCCTGAGTTCGTTG	347
4	005R	L	F: ATGAACGCAAAATACGACACA R: CTAATATCTATATCTGCTAGAGAAGATGGG	183
5	010L	IE	F: GAACCACTTTTCCATTGCCTTGC; R: GGGACGCCCTGTTGGACTTTTAC	536
6	018L	IE	F: GGTCCTTGTTCAGATTCGC R: AATCAGGGCTCTGGTTATG	347
7	019L	L	F: CTGGAGAAGAAGAATGGGAGGGG R: CTTTCGGGCAGCAGTTTTCGGTC	388
8	020L	L	F: TTAAACACTGTAGAACCAGTCTTGC R: ATGGCCTGCTATAGCCCACG	1074
9	021L	L	F: AGATGCAGGTCCGAGTTTGGTAT; R: ACCCTCCATGTGGTTCACTATGC	319
10	022R	L	F: AAGTCCATCCACGCCCACAAGGT R: TGGCAGTCTCGGGTATGTTCAGC	496
11	024L	E	F: CTTGGAGTGGAGGGACGACAGGT R: TAGCGTTTAGCGGCAACATTGGA	461
12	025L	E	F: ATCTTGACGAGCCTGGACATCTTT R: GTCCTCGGTCTTTACCAGCTACGT	474
13	026L	E	F: TTAGCACAGGTCCAACAGCTC R: ATGAGGATACTGGATCTTTTCAGC	645
14	031R	E	F: CAAGGTGTTTACGCCCAAGAGTG R: GTCAAACAGAGCCGTGTATTCCAG	427
15	036R	L	F: TGGACGACAAGTTTACTACCCT; R: TTATAAAATTTTGTACACAAACACT	255
16	037R	L	F: ATGTTTGACGCTTCGCACA; R: TCACATCCCTCCAAACAGGAC	1182
17	038R	L	F: ATGCTTATCTCATTGTCTGAGCT; R:TTAGATAATGTTAAACTTTGTCAGGA	1053
18	054L	+	F: CTCTTCTTCACAGGGGATCTC; R: ATGTATAGCGTTCGCAATTCTG	233
19	055L	L	F: CTAAAGGTCCAGTTCGTACCAA; R: ATGCATACCATTTCAGACTGG	417
20	057L	+	F: GACGGCTTGACCTCGTTGTAATC R: TTCCTAAACTCTGTTGCGAATGG	908
21	058R	E	F: GAGCGGTAGTCAGCCCATAGTGT; R: GTAGGCGTAGTGGAGCGGCGTGT	694
22	060R	E	F: CACAGTCTTTCAGCGTGACCGAT R:CCAAGAGTCTCCCAGCACATAGTAGC	737
23	065R	E	F: GGGACTCCTGACTGCCTCTGTTG; R: ACTCTTCGTGGGCTCCCTTCATC	335
24	067L	L	F: TTATTTTAATGCTAACCACAGCC; R: ATGGACGATGTCGAGTACAGAA	408
25	069L	IE	F: CTTGGCGACAGTCTTGTCATACG; R: ACCTACCCCGCAGTGATTACCTT	483
26	073L	L	F: CTAACCCTGACAGGAGGTGC R: ATGACGAGCTCAGTGTCTTTCC	1698
27	074L	L	F: CTCCTGCCCCTGCCCGCTATGAT; R: GGGATGGACAAAGAGTAAGCCGTAT	564
28	080L	IE	F: TCAGCCCATAAAGTAGGGG; R: ATGAGTGCAGGACACCTTC	318
29	082L	IE	F: CTGGGTTTGGAAGGCAGGACCAT; R: CAGGACAAGAAAGCCCGAGAAGG	702
30	087L	L	F: CCCTGCGAAGGAGTGGGTAGTCT; R: TTTCCAACGGAGCGGGCATAGAC	291
31	089L	L	F: CCGAAAGAAAAGAGGATGGGTGT; R: CCGTAATGAAACGAAACGAGGAC	225
32	092L	L	F: TGGGGATGGGACCAAACATTACA; R: GGCAAAGATTATGTGGGACTATTACG	572
33	095L	E	F: TGGCATTGCCCTTATCGGCGTAG R: CCTCACTGGATGGACCCTCACCT	247
34	096L	L	F: CACCGCCTCCTTGACGACAAACT; R: CGCAGAAACGGCATAGAGTACCAAA	465
35	099R	L	F: TGCAAGTGGGCTTCATCGGGTTA; R: TGAGACGCTCGCATTGCTTGACC	415

Table 2 (*Continued*)

No.	ORF	Temporal class	Forward primer(F) (5′ → 3′); Reverse primer (R) (5′ → 3′)	PCR product size (bp)
36	103L	E	F: GCAAGTCTCCCAGGATCTTTACA; R: GACTCCAAGAGGCACATCATACC	652
37	107R	E	F: GCCTCTTTTCCTTTGTGGAGGTG; R: AGTGGCGGCATTCTTTGCGTTCT	509
38	108L	E	F: TTAGTCCAACTCTTTGTCCA; R: ATGACAAGTGTCAAGACTATAGC	210
39	110R	+	F: ATGTGGTCTCAGTTTATCGCA; R: TTACAGAACCCTGGGGACG	687
40	111R	L	F: ATGGATGTGAGGCAATTTCTG; R: TCAAGAGAACAAGAGAGACAGGA	411

+: cDNA detected, but not determined into the temporal class.

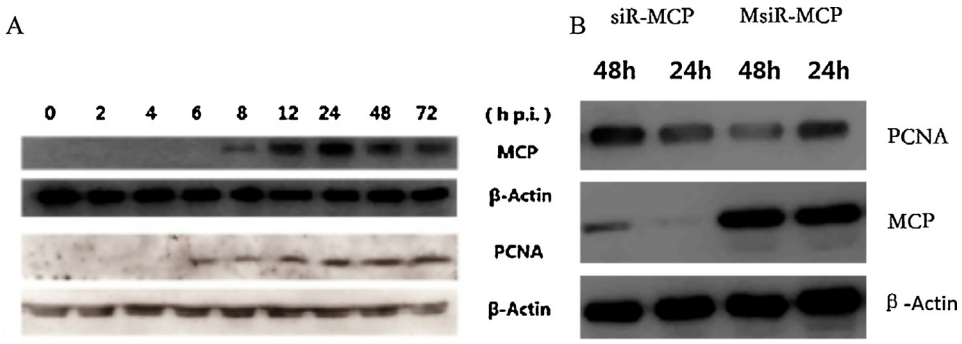

Fig. 3. WB analysis of MCP and PCNA expression after siRNA-mediated silencing. (A) Time courses of MCP and PCNA in the CGSIV infected EPC cells. (B) MCP and PCNA expression in FHM cell monolayers infected with the virus at an MOI of approximately 0.4. siR-MCP: cellular proteins of CGSIV-infected FHM cells transfected with MCP-targeted siRNA. MsiR-MCP: cellular proteins of CGSIV-infected FHM cells transfected with MsiR-MCP control.

protection for other iridovirus species in the genus *Megalocytivirus*. By contrast, the antiserum against rPCNA did not suppress virus production in CGSIV-infected FHM cells (data not shown), which suggests that PCNA does not serve as a protective antigen during CGSIV infection.

4. Discussion

CGSIV-like ranaviruses have been confirmed as emerging causative agents of disease in farmed Chinese giant salamanders in nationwide China (Dong et al., 2011b). As of this writing, the complete genome sequences of three CGSIV-like ranaviruses, including CGSIV-HN11, have been determined. Phylogenetic analysis showed that all these ranaviruses belong to the CMTV subset in the ALRV group of the genus *Ranavirus* (Chen et al., 2013; Mavian et al., 2012a). While the complete sequences of 11 ALRVs in *Ranavirus* have been determined, comprehensive studies on virion proteins of this ranaviral group are scarce. In the present study, one dimension gel-based LC ESI–MS/MS was performed to identify the virion proteins in CGSIV-HN11. A total of 40 viral proteins, including 15 core iridoviral proteins [002L, 010L, 018L, 019L(MCP), 024L, 025L,031R, 060R, 065R, 069L, 074L, 087L, 092L, 096L, and 103L], were detected in purified CGSIV-HN11. Virion proteins of 5 iridoviruses, including 3 vertebrate and 2 invertebrate iridoviruses in the family Iridoviridae, have been published. These viruses are SGIV (Song et al., 2006), ISKNV (Dong et al., 2011a), RSIV(SKIV-ZJ07) (Shuang et al., 2013), IIV6 (Ince et al., 2010), and IIV9 (Wong et al., 2011). Compared with CGSIV-HN11, 26, 11, 13, 12, and 15 orthologous viral proteins in CGSIV-HN11 have also been detected previously as virion proteins in SGIV, ISKNV, RSIV(SKIV-ZJ07), IIV6, and IIV9, respectively. Phylogenetic relationship results showed that CGSIV-HN11 and SGIV, respectively, belong to the ALRV and GLRV groups in the genus *Ranavirus*. However, ISKNV and RSIV belong to different genotypes in the genus *Megalocytivirus*, and IIV6

Table 3
siRNA sequences used in this study.

siRNA	Orientation	Sequence	Position in gene sequence
siGLO	Sense	N/A	550–568
	Antisense	N/A	
siR-MCP	Sense	CUCCCAUUCUUCUUCUCCA	
	Antisense	dTdTGAGGGUAAGAAGAAGAGGU	
MsiR-MCP	Sense	CUCCCAUUCUUCUUCUCCA	
	Antisense	dTdTG**U**G**A**GU**G**AGAAGAAGAGG**A**	

Mismatched nucleotides are bold and underlined.

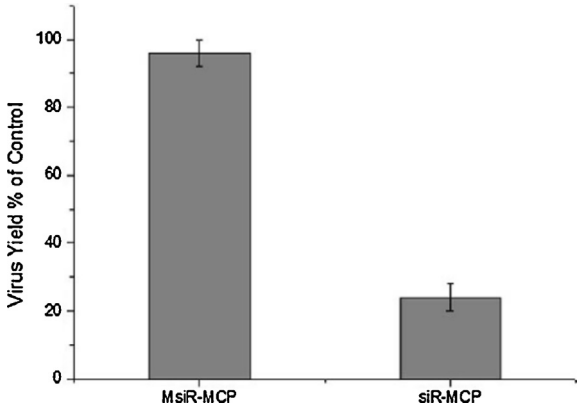

Fig. 4. Effect of virus MOI after siRNA-mediated silencing. FHM cells were transfected with MsiR-MCP and siR-MCP and followed infection with CGSIV at an MOI of 0.4 at 24 h post-transfection. At 48 hpi, the cultures were harvested and virus yields were determined by plaque assay ($n = 3$). Virus yields are expressed as a percentage of those achieved in mock-treated cultures.

and IIV9 belong to the inveterate iridovirus in family *Iridoviridae*. Thus, that SGIV proteome shares as many as 26 orthologous virion proteins with CGSIV-HN11 virion proteins is not surprising. Nine viral proteins were identified in CGSIV-HN11 in the present study and not in other studies on iridoviruses. These viral proteins include CGSIV-020L, -026L, -036R, -055L, -073L, -107R, -108L, -110R, and -111R (Table 1). The following cases are possible: (1) these proteins are differentially expressed in different virus strains and hosts; and (2) the unidentified proteins are in low abundance or have low-mass weights, which may result in very low detection levels. Not all the viral proteins identified in this work are viral structural proteins because of the confidence limitations of individual workflows (Shuang et al., 2013).

Although only one matched peptide was acquired during PCNA identification, this protein was confirmed as a viral structural protein in CGSIV-HN11 by WB analysis. Except for PCNA, 12 other virion proteins (CGSIV-005R, -020L, -026L, -036L, -038R, -055L, -057L, -073L, -080L,

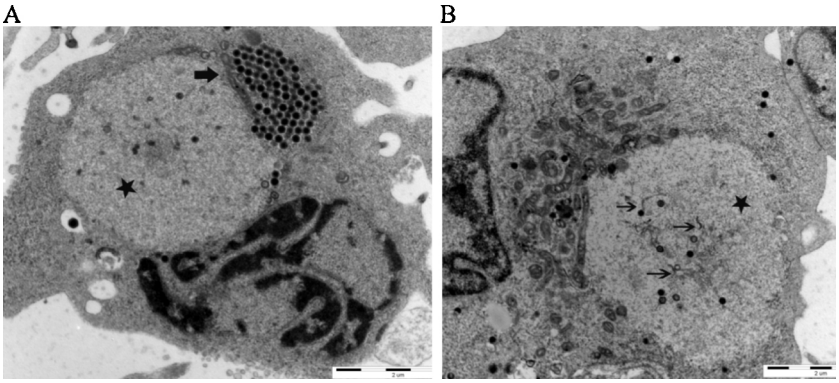

Fig. 5. TEM of MsiR-MCP and siR-MCP treated CGSIV-infected FHM cells. (A) MsiR-MCP-treated, CGSIV-infected FHM cells. (B) siR-MCP-treated CGSIV-infected FHM cells. Stars indicate the viral assembly site. Rough arrow indicates a paracrystalline array. Thin arrows indicate an aberrant structure.

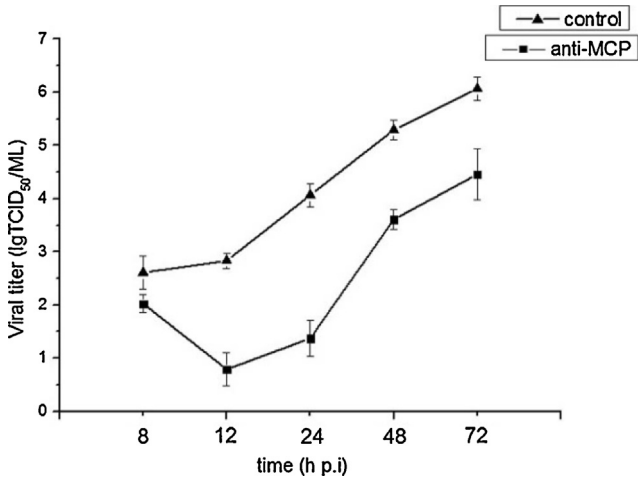

Fig. 6. Neutralization assay results showing the growth in CGSIV-infected EPC cells. An equal volume of two fold dilutions of anti-rMCP serum was added to the virus dilution (MOI = 1) and incubated at 24 °C for 1 h. Sera from non-immunized mice was included in the virus dilution analysis as controls. At the indicated time after infection, virus-infected cultures were harvested, and viral titers were determined by $TCID_{50}$ assays. All assays were analyzed in triplicate, and the data are shown in graphs, in which averages for three experiments are represented by two standard deviations (S.D.) indicated by error bars.

-092L, -108L, and -110R) also showed only one uniquely matched peptide (Table 1). Homologous proteins of seven of these proteins (CGSIV-020L, -026L, -036L, -055L, -073L, -108L, and -110R) were not detected in other iridoviral proteomes. Further confirmation should be performed using molecular biological approaches combined with immunological assays.

All transcripts of 40 virion protein genes were confirmed by RT-PCR. Transcriptional analysis combined with drug inhibition assay showed that 37 of these protein genes could be classified into three temporal kinetic classes, namely, 5 IE, 12 E, and 20 L (Table 2). The temporal classifications of MCP and PCNA were further confirmed by WB analysis. The temporal classification of CGSIV virion protein genes was compared with the available transcriptomic data from three other ranaviruses (FV3, TFV, and STIV) (Table S1). Many of the genes were conserved, but the temporal class occasionally varied, which suggests that the genes may be driven by different types of promoters. These differences imply that fine tuning of viral gene expression, DNA replication, and virion assembly varies among the different iridovirus species. Twenty ORFs were transcribed as L genes. By contrast, the majority of Chilo iridescent virus particle proteins were expressed as IE genes (Ince et al., 2013). From a general perspective, we can assume that virion protein genes belong predominantly to the L temporal class because late viral genes encode structure and scaffolding proteins or proteins that facilitate virion assembly.

CGSIV virions contain several proteins, the homologs of which were identified as envelope proteins in other iridoviruses, such as myristylated membrane protein (002L and 060R) and 095L protein. The ORF002L protein is homologous to the myristylated membrane protein in TFV, SGIV, ISKNV, RSIV(SKIV) IIV6, and IIV9 virions. The ORF060R protein is homologous to that in FV3, RGV, STIV, SGIV, ISKNV, RSIV(SKIV-ZJ07), IIV6, and IIV9 virions. These essential proteins are related to virion assembly and viral infection (He et al., 2014; Kim et al., 2010; Whitley et al., 2010). For instance, VP088 of SGIV (the CGSIV060R homolog) is a viral envelope protein, as confirmed by WB and immunoelectron microscopy. rVP088 can also bind to a 94 kDa host cell membrane protein, which suggests that VP088 functions as an attaching protein. Neutralization assay also suggested that VP088 is involved in SGIV infection (Zhou et al., 2011). The functions of crucial virion proteins in CGSIV should be studied further.

We demonstrated that CGSIV-MCP is a virion protein that is essential in infection *in vitro* using siRNA-based knockdown effects combined with anti-rMCP antibody-based neutralization test. Initially, we attempted to silence viral gene expression in EPC cells. However, we were unable to consistently demonstrate a reduction in the level of targeted messages. Failure of RNA interference in EPC could be due to the low siRNA transfection efficiency. The siRNA transfection efficiencies of EPC cells varied between 15% and 30% ($n = 4$), as estimated with fluorescent-labeled siRNA. Successful siRNA-mediated silencing in FHM cells has previously been reported (Xie et al., 2005). Thus, FHM cells were tested for CGSIV-MCP expression silencing. Successful siRNA-mediated silencing could be achieved during infection with MOIs of 1 or lower, such as 0.1 or 0.01 (Falkenhagen et al., 2009; Yamauchi et al., 2008). We attempted to reduce the MOI to ~0.1 pfu/cell for silencing MCP expression in FHM cells and found that the viral titer ($TCID_{50} = 10^{6.1}$) of CGSIV in FHM cells is much lower than that in EPC cells. Effective infection was not achieved during infection with lower MOIs, such as an MOI of 0.1. An MOI of 0.4 was experimentally confirmed as a critical dosage that can sufficiently trigger effective CGSIV infection in FHM cells (data not shown). Thus, an MOI of 0.4 is the CGSIV infection dosage suitable for inducing siRNA-mediated knockdown effect in FHM cells. Overall, knockdown of CGSIV-MCP could effectively suppress the production of CGSIV in FHM cells, as confirmed by CPE development, viral titer assays, and TEM observations. Anti-rMCP serum-based neutralization test results showed that MCP is essential during CGSIV infection, and this result is in agreement with the results of a previous study on the antiviral activity of an anti-MCR serum during STIV infection (Zhao et al., 2007).

In summary, we identified 40 viral proteins in CGSIV virions based on a proteomic approach. This paper is the first proteomic study of ALRV in the genus *Ranavirus*. Information on a temporal class of virion proteins will promote a better understanding of the assembly process of CGSIV virions. Moreover, CGSIV-MCP is confirmed as an essential virion protein in CGSIV infection *in vitro*. Our results contribute to the knowledge on virion components of CGSIV and will encourage future studies on molecular mechanisms of the ALRV pathogenesis and iridoviral disease prevention.

Acknowledgments

This research was supported by the National Basic Research Program of China under grant No. 2012CB114406; the Technology Planning Project of Guangdong Province under numbers 2011A020102002 and 2012A020800006.

Appendix A. Supplementary data

Supplementary material related to this article can be found, in the online version, at http://dx.doi.org/10.1016/j.vetmic.2014.05.009.

References

Chen, Z., Gui, J., Gao, X., Pei, C., Hong, Y., Zhang, Q., 2013. Genome architecture changes and major gene variations of *Andrias davidianus* ranavirus (ADRV). Vet. Res. 44, 101.

Chinchar, V.G., Waltzek, T.B., 2014. Ranaviruses: not just for frogs. PLoS Pathog. 10, e1003850.

Chinchar, V.G., Yu, K.H., Jancovich, J.K., 2011. The molecular biology of frog virus 3 and other iridoviruses infecting cold-blooded vertebrates. Viruses 3, 1959–1985.

Dong, C., Xiong, X., Luo, Y., Weng, S., Wang, Q., He, J., 2013. Efficacy of a formalin-killed cell vaccine against infectious spleen and kidney necrosis virus (ISKNV) and immunoproteomic analysis of its major immunogenic proteins. Vet. Microbiol. 162, 419–428.

Dong, C.F., Xiong, X.P., Shuang, F., Weng, S.P., Zhang, J., Zhang, Y., Luo, Y.W., He, J.G., 2011a. Global landscape of structural proteins of infectious spleen and kidney necrosis virus. J. Virol. 85, 2869–2877.

Dong, W., Zhang, X., Yang, C., An, J., Qin, J., Song, F., Zeng, W., 2011b. Iridovirus infection in Chinese giant salamanders, China, 2010. Emerg. Infect. Dis. 17, 2388–2389.

Falkenhagen, A., Heinrich, J., Moelling, K., 2009. Short hairpin-loop-structured oligodeoxynucleotides reduce HSV-1 replication. Virol. J. 6, 43.
Geng, Y., Wang, K.Y., Zhou, Z.Y., Li, C.W., Wang, J., He, M., Yin, Z.Q., Lai, W.M., 2011. First report of a ranavirus associated with morbidity and mortality in farmed Chinese giant salamanders (*Andrias davidianus*). J. Comp. Pathol. 145, 95–102.
He, J.G., Lu, L., Deng, M., He, H.H., Weng, S.P., Wang, X.H., Zhou, S.Y., Long, Q.X., Wang, X.Z., Chan, S.M., 2002. Sequence analysis of the complete genome of an iridovirus isolated from the tiger frog. Virology 292, 185–197.
He, L.B., Ke, F., Wang, J., Gao, X.C., Zhang, Q.Y., 2014. *Rana grylio* virus (RGV) envelope protein 2L: subcellular localization and essential roles in virus infectivity revealed by conditional lethal mutant. J. Gen. Virol. 95, 679–690.
Huang, Y., Huang, X., Liu, H., Gong, J., Ouyang, Z., Cui, H., Cao, J., Zhao, Y., Wang, X., Jiang, Y., Qin, Q., 2009. Complete sequence determination of a novel reptile iridovirus isolated from soft-shelled turtle and evolutionary analysis of *Iridoviridae*. BMC Genomics 10, 224.
Ince, I.A., Boeren, S.A., van Oers, M.M., Vervoort, J.J., Vlak, J.M., 2010. Proteomic analysis of *Chilo iridescent* virus. Virology 405, 253–258.
Ince, I.A., Ozcan, K., Vlak, J.M., van Oers, M.M., 2013. Temporal classification and mapping of non-polyadenylated transcripts of an invertebrate iridovirus. J. Gen. Virol. 94, 187–192.
Jancovich, J.K., Bremont, M., Touchman, J.W., Jacobs, B.L., 2010. Evidence for multiple recent host species shifts among the Ranaviruses (family *Iridoviridae*). J. Virol. 84, 2636–2647.
Jancovich, J.K., Chinchar, V.G., Hyatt, A., Miyazaki, T., Williams, T., Zhang, Q.Y., 2012. Family *Iridoviridae*. In: King, A.M.Q., Adams, M.J., Carstens, E.B., Lefkowitz, E.J. (Eds.), Virus Taxonomy: Ninth Report of the International Committee on Taxonomy of Viruses. Elsevier Academic Press, San Diego, CA, pp. 193–210.
Jancovich, J.K., Mao, J., Chinchar, V.G., Wyatt, C., Case, S.T., Kumar, S., Valente, G., Subramanian, S., Davidson, E.W., Collins, J.P., Jacobs, B.L., 2003. Genomic sequence of a ranavirus (family *Iridoviridae*) associated with salamander mortalities in North America. Virology 316, 90–103.
Jiang, Y.L., Zhang, M., Jing, H.L., Gao, L.Y., 2011. [Isolation and characterization of an iridovirus from sick giant salamander (*Andrias davidianus*)]. Bing Du Xue Bao 27, 274–282.
Kim, Y.S., Ke, F., Lei, X.Y., Zhu, R., Zhang, Q.Y., 2010. Viral envelope protein 53R gene highly specific silencing and iridovirus resistance in fish Cells by AmiRNA. PLoS One 5, e10308.
Lei, X.Y., Ou, T., Zhu, R.L., Zhang, Q.Y., 2012. Sequencing and analysis of the complete genome of *Rana grylio* virus (RGV). Arch. Virol. 157, 1559–1564.
Mavian, C., Lopez-Bueno, A., Balseiro, A., Casais, R., Alcami, A., Alejo, A., 2012a. The genome sequence of the emerging common midwife toad virus identifies an evolutionary intermediate within ranaviruses. J. Virol. 86, 3617–3625.
Mavian, C., Lopez-Bueno, A., Fernandez Somalo, M.P., Alcami, A., Alejo, A., 2012b. Complete genome sequence of the European sheatfish virus. J. Virol. 86, 6365–6366.
Reed, L.J., Muench, H., 1938. A simple method of estimating fifty percent endpoints. Am. J. Hyg. 27, 493–497.
Shuang, F., Luo, Y., Xiong, X., Weng, S., Li, Y., He, J., Dong, C., 2013. Virions proteins of an RSIV-type megalocytivirus from spotted knifejaw *Oplegnathus punctatus* (SKIV-ZJ07). Virology 437, 27–37.
Song, W., Lin, Q., Joshi, S.B., Lim, T.K., Hew, C.L., 2006. Proteomic studies of the Singapore grouper iridovirus. Mol. Cell. Proteomics 5, 256–264.
Song, W.J., Qin, Q.W., Qiu, J., Huang, C.H., Wang, F., Hew, C.L., 2004. Functional genomics analysis of Singapore grouper iridovirus: complete sequence determination and proteomic analysis. J. Virol. 78, 12576–12590.
Tan, W.G., Barkman, T.J., Gregory Chinchar, V., Essani, K., 2004. Comparative genomic analyses of frog virus 3, type species of the genus *Ranavirus* (family *Iridoviridae*). Virology 323, 70–84.
Tsai, C.T., Ting, J.W., Wu, M.H., Wu, M.F., Guo, I.C., Chang, C.Y., 2005. Complete genome sequence of the grouper iridovirus and comparison of genomic organization with those of other iridoviruses. J. Virol. 79, 2010–2023.
Whitley, D.S., Sample, R.C., Sinning, A.R., Henegar, J., Chinchar, V.G., 2011. Antisense approaches for elucidating ranavirus gene function in an infected fish cell line. Dev. Comp. Immunol. 35, 937–948.
Whitley, D.S., Yu, K., Sample, R.C., Sinning, A., Henegar, J., Norcross, E., Chinchar, V.G., 2010. Frog virus 3 ORF 53R, a putative myristoylated membrane protein, is essential for virus replication in vitro. Virology 405, 448–456.
Whittington, R.J., Becker, J.A., Dennis, M.M., 2010. Iridovirus infections in finfish—critical review with emphasis on ranaviruses. J. Fish Dis. 33, 95–122.
Wong, C.K., Young, V.L., Kleffmann, T., Ward, V.K., 2011. Genomic and proteomic analysis of invertebrate iridovirus type 9. J. Virol. 85, 7900–7911.
Xie, J., Lu, L., Deng, M., Weng, S., Zhu, J., Wu, Y., Gan, L., Chan, S.M., He, J., 2005. Inhibition of reporter gene and Iridovirus-tiger frog virus in fish cell by RNA interference. Virology 338, 43–52.
Yamauchi, Y., Kiriyama, K., Kimura, H., Nishiyama, Y., 2008. Herpes simplex virus induces extensive modification and dynamic relocalisation of the nuclear mitotic apparatus (NuMA) protein in interphase cells. J. Cell Sci. 121, 2087–2096.
Zhao, Z., Teng, Y., Liu, H., Lin, X., Wang, K., Jiang, Y., Chen, H., 2007. Characterization of a late gene encoding for MCP in soft-shelled turtle iridovirus (STIV). Virus Res. 129, 135–144.
Zhou, S., Wan, Q., Huang, Y., Huang, X., Cao, J., Ye, L., Lim, T.K., Lin, Q., Qin, Q., 2011. Proteomic analysis of Singapore grouper iridovirus envelope proteins and characterization of a novel envelope protein VP088. Proteomics 11, 2236–2248.